IAC-24-C2,IP,115,x87008

Functional behaviour of an innovative complex Nitinol structure for space applications manufactured by Selective Laser Melting

Biasutti T.[a]*, Bettini P.[b], Grande A. M.[c] , Colosimo B.M.[d], Sala G.[e], Nespoli A[f].

[a] *Department of Mechanical Engineering, Politecnico di Milano, via La Masa 1, 20156 Milan, Italy, tiziana.biasutti@polimi.it*
[b] *Department of Aerospace Engineering, Politecnico di Milano, via La Masa 34, 20156 Milan, Italy, paolo.bettini@polimi.it*
[c] *Department of Aerospace Engineering, Politecnico di Milano, via La Masa 34, 20156 Milan, Italy, antoniomattia.grande@polimi.it*
[d] *Department of Mechanical Engineering, Politecnico di Milano, via La Masa 1, 20156 Milan, Italy, biancamaria.colosimo@polimi.it*
[e] *Department of Aerospace Engineering, Politecnico di Milano, via La Masa 34, 20156 Milan, Italy, giuseppe.sala@polimi.it*
[f] *National Research Council, Institute of Condensed Matter Chemistry and Technologies for Energy (CNR-ICMATE), via G. Previati 1/e, 23900 Lecco, Italy, adelaide.nespoli@cnr.it*
* Corresponding Author

Abstract

NiTi alloy is a smart material characterized by two effects, “Shape Memory Effect” and “Pseudoelastic Effect”. It is one of the most widely used Shape Memory Alloys (SMA) and its properties can be interesting for aeronautical and space applications. In particular, for the latter field, the usage of NiTi can lead to weight reduction and increased reliability, since it would eliminate the need for complex mechanisms. The Shape Memory Effect allows to use NiTi for actuation, while the Psudoelastic Effect enables the material to recover large deformations and can be employed to provide structural damping. Currently, the main limit to the widespread adoption of NiTi is its poor workability with conventional technologies, and for this reason, the development of new production technologies, such as Additive Manufacturing (AM), is of great interest to research.

This work focuses on the study of the two effects of SMA in an innovative complex structure with origami geometry. The origami samples were fabricated through Laser Powder Bed Fusion (LPBF), an AM process that uses a laser beam to selectively melt layers of micrometric metal powders. The LPBF process parameters were established through a prior investigation on simple-shaped specimens aimed to guarantee the material’s performance and minimize the occurrence of defects. The studied geometry presents an intrinsic suitability for energy absorption, so when SMA are employed in the pseudoelastic regime, the material functionality increases the structural damping performances. Likewise, thanks to the shape memory effect, once the structure is heated over a certain threshold the pre-strained structure recovers its initial shape, thus obtaining a deployable structure.

Thermal analysis and thermo-mechanical tests were used to investigate the overall performance of the origami structure. Once assessed the phase transformation temperatures, the structure was analysed to investigate separately the pseudoelastic and shape memory effects.

Keywords: NiTi, Additive Manufacturing, Laser Powder Bed Fusion, origami structure, Shape Memory Effect, Pseudoelastic Effect

Acronyms/Abbreviations

SMA	Shape Memory Alloys
AM	Additive Manufacturing
L-PBF	Laser-Powder Bed Fusion
SME	Shape Memory Effect
PE	Pseudoelastic Effect
SLM	Selective Laser Melting
DSC	Differential Scanning Calorimetry
M_F	Martensite Finish Temperature
M_S	Martensite Start Temperautre
A_F	Austenite Finish Temperature
SIM	Stress Induced Martensite

1. Introduction

The space environment is always looking for innovative applications and materials to improve the performances of the systems, increase reliability, and reduce weight. NiTi is a Shape Memory Alloys (SMA) that shows fascinating performances and it is of interest for space applications due to its functionality [1, 2]. NiTi indeed exhibits two effects that can be triggered by

application of external stresses or variation of temperature. These behaviours are possible thanks to the two stable phases of the material: austenite phase, stable at high temperatures, and martensite phase, stable at low temperatures. The transformation from one phase to the other allows to obtain the two effects of the material, called Shape Memory Effect (SME) and Pseudoelastic Effect (PE). The SME allows to recover the initial shape of the structure through deformation of martensite phase and then heating the material at higher temperatures to recover the austenite state and the original shape [3, 4]. This effect can be used to produce motion and it is useful in space environments since it allows to design, for example, low weight movable systems. On the other hand, the second effect, PE, allows the material to recover high strain, up to 8%, through a thermo-mechanical hysteretic behaviour and without permanent deformations [5]. This behaviour is suitable for damping applications. In this case the material is initially in austenite phase and due to the application of external load, it transforms to stress induced martensite [6]. After the removing of the load it comes back to austenite phase. Depending on the Ni/Ti ratio, NiTi can present SME or PE at different temperatures, and this makes it suitable for space applications at different thermal conditions. Moreover, it is possible to vary its mechanical properties by varying the working temperature, or vice versa, setting the temperature to have specific mechanical behaviours.

The biggest limitations of NiTi, which reduced its widespread diffusion, are the challenges related to the traditional technologies to manufacture complex structures. This led to the possibility to obtain only simple shapes structures, as wires, springs, tubes or plates. This difficulty guided the research world to source for new manufacturing technologies to produce innovative and complex shapes, that cannot be manufactured through traditional technologies. One of the technologies on which the research is focusing is Selective laser Melting (SLM), that is a Laser Powder Bed Fusion (L-PBF) technique [7] that nowadays has received particular attention for NiTi alloy.

Most of the studies on the printability of NiTi through SLM are focused mainly on the correlation of the printing parameters to the Ni and Ti content in the printed part [8, 9]. The manufacturing process indeed, leads to variations of Nickel and Titanium atomic percentages and the consequent variation of mechanical and thermal properties of the material [10]. A reduction of the Ni percentage, for example, leads to an increase in the transformation temperatures of the material from austenite to martensite and vice versa, with the consequent variation of the working condition of the material.

Moreover, high interest was placed on pseudoelastic effect [11, 12], especially for example for biomedical applications. In this case the most studied structures are the lattice ones [13].

For what concern the shape memory effect instead, few works focused on that and the majority considered only the shape recovery of simple shape structures. Nevertheless, some works such as [14, 15] considered more complex shapes as chiral and honeycomb lattice structures and analysed their ability to absorb energy and recover the initial shape after heating at high temperatures. In both works the high potential of NiTi structures was demonstrated.

In this research, an origami structure was manufactured and completely characterized. The origami structures have been of big interest in space field in recent years due to their possibility to be stored in small volumes. The present work starts from a previously analysed polymer origami structure [16]. In the current research, the origami structure was manufactured in NiTi, adding to the structure also the functionality of SMA. Furthermore, the structure was characterized considering both the actuation and the pseudoelastic effect.

2. Material and methods

The origami structure was manufactured in a reduced building volume through a Renishaw AM400 (Figure 1). The printing parameters are reported in Table 1 and were defined in previous work, optimizing the presence of defects and the functionality of the material [10]. The powder (Nanoval) has 50.8 at. % of Ni content and size between 20 μm and 50 μm.

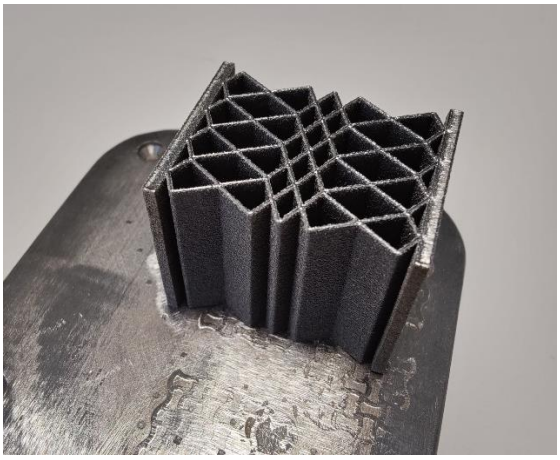

Fig. 1: Manufactured origami structure before removing from the building platform

Table 1. Printing Parameters used for the manufacturing of the origami structure

Laser Power (W)	Point distance (µm)	Exposure time (µs)	Layer thickness (µm)	Hatch distance (µm)
100	60	240	30	120

Samples were removed from the building platform by electro-discharge machining and then they were heat treated at 950 °C for 5.5 h and water quench, followed by aging at 450 °C for 15 minutes and, also in this case, water quench.

Differential Scanning Calorimetry (DSC) was carried out on heat treated representative beams that show diameters close to the size of the origami structure's walls (i.e. 0.5 mm and 0.7 mm). DSC was performed from – 120 °C to 120 °C with a heating/cooling rate of 10 °C/min. From DSC curves the transformation temperatures were identified by applying the tangent method.

Finally, the mechanical characterization in force controlled mode, was accomplished through an Instron Electropuls E3000 at different temperatures to assess the functionality of the material. The characterization of the martensite phase was performed at martensite finish temperature M_F through loading/unloading cycles from 600 N to 1000 N and, after the test, heating the structure from M_F to 80 °C. At M_F also the failure of the sample was analysed. The characterization of the austenite phase instead was assessed at A_F + 10 °C, through three loading/unloading cycles from 600 N to the failure of the sample.

Moreover, the actuation at room temperature was performed by varying the applied load in the range from 600 N to 1200 N, and by heating the loaded structure from room temperature to 80°C. The stroke at each load was measured through ImageJ software.

3. Results

The results of DSC analyses performed on 0.5 mm and 0.7 mm beams are shown in Figure 2. The transformation temperatures after the heat treatment are similar for the two structures. The 0.7 mm beam presents a reverse transformation with multiple picks, contrary to the 0.5 mm beam.

According to the DSC graphs carried out, it can be said that the phase transformation temperature of martensite finish and martensite start are, M_F – 55 °C for 0.5 mm and – 43 ° for 0.7 mm diameter, and M_S – 32 °C and -31 °C, for 0.5 mm and 0.7 mm diameters respectively. For what concern the transformation from martensite to austenite, the austenite start temperature are 7 °C for 0.5 mm and 2 °C for 0.7 mm, and finally the austenite finish temperatures are 30°C in both cases.

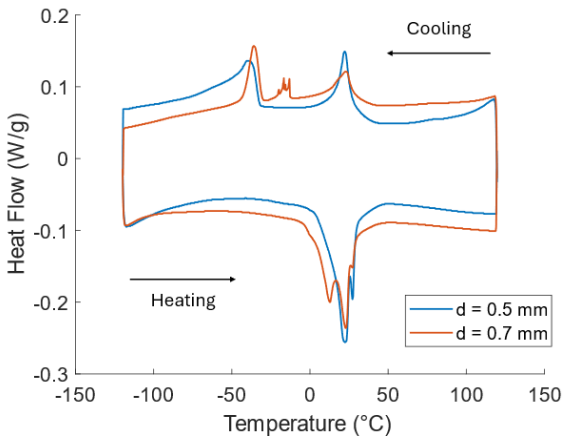

Fig. 2: DSC curves of 0.5 mm and 0.7 mm beams manufactured to represent origami structure walls

3.1 Martensite

The mechanical test on martensite at 1000 N is depicted in Figure 3. The picture also reports the photographs of the deformed origami structures at -40°C and of the recovered origami shape at 80°C. Furthermore, Table 2 lists the strokes of the origami structure under different loads. The maximum value obtained for 1000 N test, is 2.85 mm displacement.

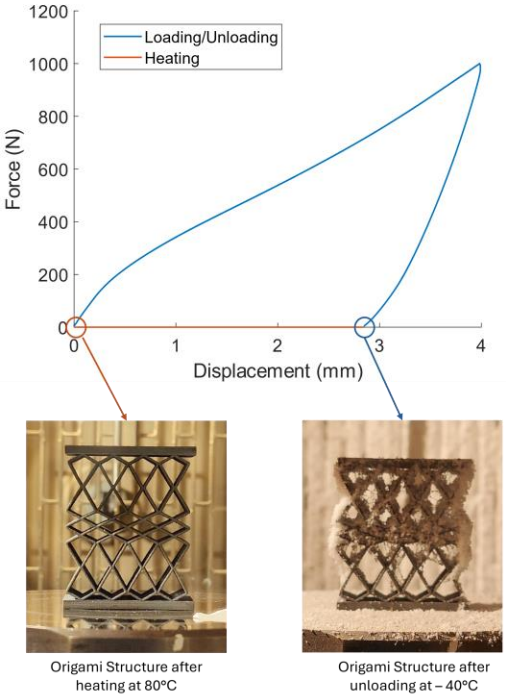

Fig. 3: Loading and unloading cycles at 1000 N at M_F and detail of structure after unloading at -40°C and after heating at 80°C

Table 2: Recovered deformation that the origami structure shows after heating from -40°C to 80°C at different loads

Load (N)	Recovered Deformation (mm)
600	1.41
650	1.62
700	1.84
800	2.18
900	2.49
1000	2.85

The last characterization performed of the martensite phase is a failure study. As shown in Figure 4, after failure, the structure shows an evident deformation in the central region, as well as a deformation of the longer arms near the two bases. The failure is reached at displacement of 10 mm and loads of 1950 N. Figure 4 depicts the structure after the failure in two points in the longer arms, and the structure after heating from – 40 °C to 80 °C. As is possible to see, except for the two failure points, the recovery of the initial origami shape is almost complete.

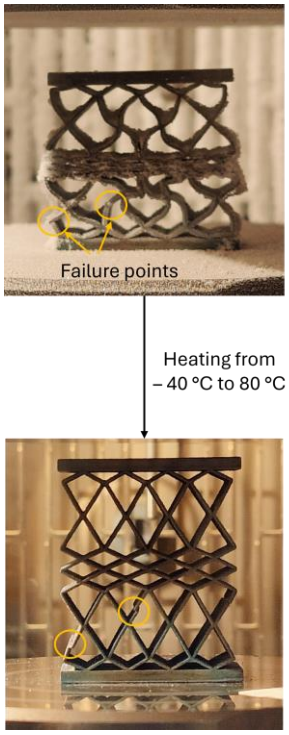

Fig. 4: Structure at M_F after failure at 1950 N and after heating to 80°C. Yellow marks highlight the failure point before and after heating

3.2 Austenite AF + 10°C

Figure 5 represents the three loading-unloading cycles performed at loads of 1000 N and 1400 N. It can be noticed that up to 800 N the origami cell exhibits a quasi-elastic behaviour. Beyond this load, the Stress Induced Martensite (SIM) begins to nucleate. Table 3 lists the residual displacements and the loss factors calculated for each applied load. It is possible to observe that as the load increase, the residual displacement and the loss factor increase as well. The highest loss factor achieved at 1400 N is 0.0414.

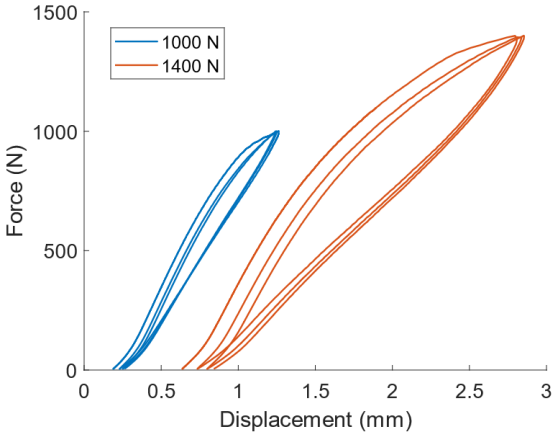

Fig. 5: Pseudoelastic curves at A_F + 10°C. Three cycles at 1000 N and 1400 N

Table 3: Loss factor and residual displacements for each loading conditions tested at A_F + 10°C

Load (N)	Loss Factor (-)	Residual Displacement (mm)
600	0.0101	0.072
700	0.0116	0.099
800	0.0148	0.135
900	0.0191	0.189
1000	0.0230	0.262
1100	0.0272	0.357
1200	0.0318	0.475
1300	0.0365	0.638
1400	0.0414	0.841

The failure of the austenite structure is reached at 1500 N for a displacement of 4 mm. As it is possible to see in Figure 6, the failure starts in correspondence of the central area. In contrast to what observed in the martensitic structure, the two areas near the bases remain undamaged.

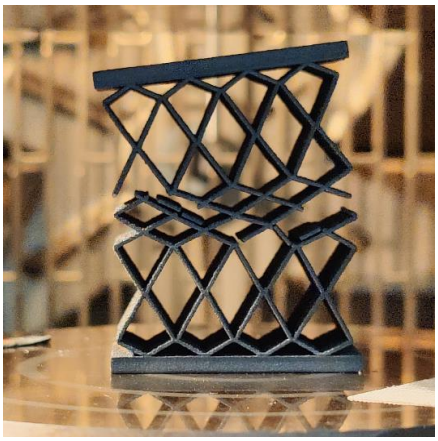

Fig. 6: Origami structure after failure in the austenite phase

3.2 Actuation at Room Temperature

The actuation of the structure is tested at room temperature and for loads from 600 N to 1200 N. The corresponding residual displacement and stroke measured at each loading condition are reported in Figure 7. The maximum stroke obtained at the conditions studied is 2.0 mm for the applied load of 1200 N.

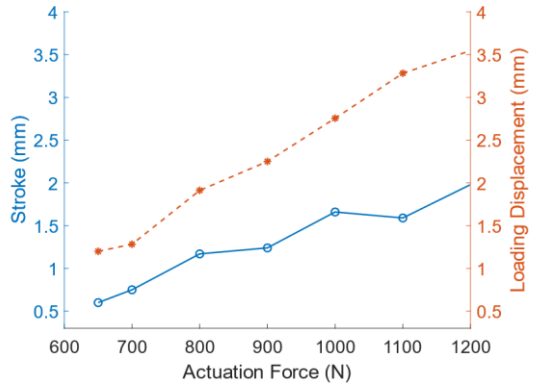

Fig. 7: Stroke and displacement obtained during loading at different actuation forces at room temperature

5. Discussion

The DSC results allow to define the test temperature of the three mechanical tests. The two rods analysed show almost equal transformation temperatures and allow to suppose that the composition of the structure is homogeneous. It is consequently possible to consider the phase transformation temperatures of the origami structure equal to the thin beams' ones.

The M_F test characterised the martensite phase and its ability to recover the initial shape after heating at temperatures higher than A_F. In this case, the structure demonstrated a good ability to completely recover displacement, up to 2.85 mm, and does not exhibit undesired damage. This ability is partially confirmed also in the failure test, in which after the failure of the structure, the sample still recovers the original shape in the undamaged parts of the sample.

Also, the test of the pseudoelastic effect at A_F + 10°C confirmed the capability of the origami geometry manufactured in NiTi to recover the imposed deformation. Indeed, the test at 1400 N shows a residual displacement of only 0.8 mm. The loss factor confirmed the good damping ability of the geometry combined with the material functionality. The maximum loss factor of 0.0414 represents a good result, comparable to the one associated with the material itself with a simple geometry manufacture with the same printing parameters [10]. It is also a good result if compared to other literature values [17].

Furthermore, the actuation shows the possibility of having a stroke of 2.0 mm under loading of 1200 N. The stroke obtained compared to the displacement imposed at the two loads is 83%. It is possible to suppose that all the displacement not related to the stroke of the actuator, is associated with the elastic deformation of the structure and it is recovered after the unloading of the sample.

6. Conclusions

The three testing conditions analysed in this work correspond to three possible space applications of the structure: shock absorber at M_F, damping at A_F + 10°C, and systems actuation at room temperature. For all these applications, the origami structure shows good performances.

The SLM technology allows to manufacture the origami geometry in NiTi, combining the functionality of the material and the advantages of AM. The obtained performance demonstrated the good functionality of the material, with selected printing parameters, and of the geometry. Indeed, it is observed a completely shape recovery up to 1000 N at low temperature, loss factor of 0.0414 for load of 1200 N at A_F +10° C and actuation stroke of 2.00 mm at room temperatures. These results are of great interest since confirm the possibility of using SLM for NiTi, maintaining its performance, and encouraging to continue the study of this technology for future engineering applications.

Acknowledgements

The authors want to acknowledge the Italian Space Agency (ASI) for the support. Grant agreement 2018-5-HH.0.

References

[1] G. Costanza and M. E. Tata, "Shape memory alloys for aerospace, recent developments, and new applications: A short review," Apr. 01, 2020, *MDPI AG*. doi: 10.3390/MA13081856.

[2] V. Malik, S. Srivastava, S. Gupta, V. Sharma, M. Vishnoi, and T. G. Mamatha, "A novel review on shape memory alloy and their applications in extraterrestrial roving missions," in *Materials Today: Proceedings*, Elsevier Ltd, 2020, pp. 4961–4965. doi: 10.1016/j.matpr.2020.12.860.

[3] T. Biasutti, D. Rigamonti, E. Casciaro, A. M. Grande, and P. Bettini, "Hingeless arm for space robotics actuated through shape memory alloys," *Bioinspir Biomim*, vol. 19, no. 1, Jan. 2024, doi: 10.1088/1748-3190/ad1069.

[4] A. Airoldi, D. Rigamonti, G. Sala, P. Bettini, E. Villa, and A. Nespoli, "Development of an actuated corrugated laminate for morphing structures," *Aeronautical Journal*, vol. 125, no. 1283, pp. 180–204, Jan. 2021, doi: 10.1017/aer.2020.70.

[5] A. Nespoli, D. Rigamonti, M. Riva, E. Villa, and F. Passaretti, "Study of pseudoelastic systems for the design of complex passive dampers: Static analysis and modeling," *Smart Mater Struct*, vol. 25, no. 10, Sep. 2016, doi: 10.1088/0964-1726/25/10/105001.

[6] F. M. Weafer, Y. Guo, and M. S. Bruzzi, "The effect of crystallographic texture on stress-induced martensitic transformation in NiTi: A computational analysis," *J Mech Behav Biomed Mater*, vol. 53, pp. 210–217, Jan. 2016, doi: 10.1016/j.jmbbm.2015.08.023.

[7] K. Kubášová *et al.*, "A Review on Additive Manufacturing Methods for NiTi Shape Memory Alloy Production," *Materials*, vol. 17, no. 6, p. 1248, Mar. 2024, doi: 10.3390/ma17061248.

[8] J. N. Zhu *et al.*, "Controlling microstructure evolution and phase transformation behavior in additive manufacturing of nitinol shape memory alloys by tuning hatch distance," *J Mater Sci*, vol. 57, no. 10, pp. 6066–6084, Mar. 2022, doi: 10.1007/s10853-022-07007-z.

[9] M. Zamani, M. Kadkhodaei, M. Badrossamay, and E. Foroozmehr, "Adjustment of the scan track spacing and linear input energy to fabricate dense, pseudoelastic Nitinol shape memory alloy parts by selective laser melting," *J Intell Mater Syst Struct*, vol. 33, no. 13, pp. 1719–1730, Aug. 2022, doi: 10.1177/1045389X211063948.

[10] T. Biasutti *et al.*, "3D printing of shape memory Alloys for complex architectures of smart structures," *Acta Astronaut*, vol. 221, pp. 206–217, 2024, doi: https://doi.org/10.1016/j.actaastro.2024.05.024.

[11] S. Saedi *et al.*, "Shape memory response of porous NiTi shape memory alloys fabricated by selective laser melting," *J Mater Sci Mater Med*, vol. 29, no. 4, Apr. 2018, doi: 10.1007/s10856-018-6044-6.

[12] A. Nespoli *et al.*, "Towards an understanding of the functional properties of NiTi produced by powder bed fusion," *Progress in Additive Manufacturing*, vol. 6, no. 2, pp. 321–337, May 2021, doi: 10.1007/s40964-020-00155-1.

[13] E. Farber *et al.*, "TiNi Alloy Lattice Structures with Negative Poisson's Ratio: Computer Simulation and Experimental Results," *Metals (Basel)*, vol. 12, no. 9, Sep. 2022, doi: 10.3390/met12091476.

[14] X. Li *et al.*, "3D Chiral Energy-Absorbing Structures with a High Deformation Recovery Ratio Fabricated via Selective Laser Melting of the NiTi Alloy," *ACS Appl Mater Interfaces*, vol. 15, no. 46, pp. 53746–53754, Nov. 2023, doi: 10.1021/acsami.3c13270.

[15] Z. Yu *et al.*, "Shock-Resistant and Energy-Absorbing Properties of Bionic NiTi Lattice Structure Manufactured by SLM," *J Bionic Eng*, vol. 19, no. 6, pp. 1684–1698, Nov. 2022, doi: 10.1007/s42235-022-00221-0.

[16] M. Mehrpouya, T. Edelijn, M. Ibrahim, A. Mohebshahedin, A. Gisario, and M. Barletta, "Functional Behavior and Energy Absorption Characteristics of Additively Manufactured Smart Sandwich Structures," *Adv Eng Mater*, vol. 24, no. 9, Sep. 2022, doi: 10.1002/adem.202200677.

[17] A. Nespoli, P. Bettini, E. Villa, G. Sala, F. Passaretti, and A. M. Grande, "A Study on Damping Property of NiTi Elements Produced by Selective Laser-Beam Melting," *Adv Eng Mater*, vol. 23, no. 6, Jun. 2021, doi: 10.1002/adem.202001246.